Journal Pre-proof

Integrated T-Cell Enrichment, Static Transduction, and Expansion in Gas-Permeable Bioreactors for Adoptive Cell Therapy

Nikolaos Gkitsas-Long , Aidan J Retherford , Carely Fowler , Dorota D Klysz , Andrew Scheffler , Dan Fick , Janette Mata Alcazar , Annie K Brown , Casey Carr , Michelle Monje , Steven A Feldman , Crystal L Mackall , Ramya H Tunuguntla

PII: S1465-3249(26)00931-X
DOI: https://doi.org/10.1016/j.jcyt.2026.102970
Reference: JCYT 102970

To appear in: *Cytotherapy*

Received date: 5 June 2026
Accepted date: 21 July 2026

Please cite this article as: Nikolaos Gkitsas-Long , Aidan J Retherford , Carely Fowler , Dorota D Klysz , Andrew Scheffler , Dan Fick , Janette Mata Alcazar , Annie K Brown , Casey Carr , Michelle Monje , Steven A Feldman , Crystal L Mackall , Ramya H Tunuguntla , Integrated T-Cell Enrichment, Static Transduction, and Expansion in Gas-Permeable Bioreactors for Adoptive Cell Therapy, *Cytotherapy* (2026), doi: https://doi.org/10.1016/j.jcyt.2026.102970

Integrated T-Cell Enrichment, Static Transduction, and Expansion in Gas-Permeable Bioreactors for Adoptive Cell Therapy

Nikolaos Gkitsas-Long[1,*], Aidan J Retherford[1,*], Carely Fowler[1], Dorota D Klysz[1], Andrew Scheffler[5], Dan Fick[6], Janette Mata Alcazar[1], Annie K Brown[1], Casey Carr[1], Michelle Monje[1,2], Steven A Feldman[1,‡], Crystal L Mackall[1,2,3,4,‡], Ramya H Tunuguntla[1,‡,¶]

[1]Stanford Center for Cancer Cell Therapy, Stanford Cancer Institute, Stanford University, Stanford, CA

[2]Division of Pediatric Hematology/Oncology/Stem Cell Transplant and Regenerative Medicine, Department of Pediatrics, Stanford University, Stanford, CA USA

[3]Parker Institute for Cancer Immunotherapy, San Francisco, CA, USA

[4]Division of Stem Cell Transplantation and Cell Therapy, Department of Medicine, Stanford University, Stanford, CA, USA

[5]ScaleReady, Saint Paul, Minnesota, USA

[6]Wilson Wolf Manufacturing Corporation, Saint Paul, Minnesota, USA

[*] These authors contributed equally

‡These authors jointly supervised this work

[¶] Corresponding author, ramyajsb@stanford.edu

ABSTRACT

Background aims: Broader access to autologous chimeric antigen receptor (CAR) T-cell therapy is limited by costly, device-bound manufacturing workflows and reliance on dedicated instrumentation for discrete unit operations, including T-cell enrichment and culture. These constraints affect academic, decentralized and high-throughput centralized manufacturing programs. We developed a closed-system CAR T-cell manufacturing workflow centered on a gas-permeable G-Rex bioreactor platform that enables direct in-vessel $CD4^+/CD8^+$ T-cell enrichment, static viral transduction and expansion without requiring a separate standalone enrichment device or spinoculation hardware.

Methods: Key unit operations of a G-Rex-based GD2 CAR T-cell manufacturing process were optimized, including RetroNectin-mediated static retroviral transduction, coating concentration and timing, and media-exchange strategy. T-cell phenotype and functional potency were characterized longitudinally throughout the 7-day culture period. The optimized workflow was translated to a manufacturing-scale G-Rex 100M-CS process incorporating a newly developed, previously unpublished method for direct in-vessel $CD4^+/CD8^+$ magnetic enrichment using detachable beads and a prototype SepaRex magnetic base. At-scale products from three healthy donors were assessed for enrichment performance, transduction efficiency, expansion, viability, phenotype, cytokine secretion and tumor-cell killing, and benchmarked against historical products manufactured using a clinically validated CliniMACS Prodigy-based GD2 CAR T-cell process.

Results: Retronectin-coated G-Rex cultures supported efficient static retroviral transduction without spinoculation, and media exchange between 24 and 96 hours post-transduction did not significantly affect final yield or viability. Direct in-vessel $CD4^+/CD8^+$ enrichment achieved 61.6 ± 8.6% recovery and 87.2 ± 7.9% purity. At manufacturing scale, the integrated workflow generated GD2 CAR T cells with 62.3 ± 5.1% transduction efficiency, 26.8 ± 4.7-fold expansion, >94% viability and >96% $CD3^+$ T-cell purity. Final products retained central memory features, secreted cytokines and mediated cytotoxicity against GD2-expressing tumor targets, with manufacturing performance comparable to the historical Prodigy-based process.

Conclusions: This closed, scalable and cost-conscious G-Rex-based workflow integrates T-cell enrichment, activation, static viral transduction and expansion within a single bioreactor-centered process. By eliminating dedicated enrichment instrumentation and reducing reliance on highly automated, device-bound culture systems, this bioreactor-centered platform may support flexible CAR T-cell manufacturing across academic, decentralized, and high-throughput centralized settings.

Key Words: CAR T cells, scalable cell therapy manufacturing, in-vessel enrichment, Retronectin, static transduction

Introduction

Autologous cell therapies, including chimeric antigen receptor (CAR) and T cell receptor (TCR) engineered T cells, have transformed treatment paradigms for hematologic malignancies and are under active investigation across an expanding range of solid tumor and non-oncology indications [1-3]. Despite this clinical progress, manufacturing cost and complexity remains a central bottleneck limiting broader patient access. Persistent challenges include constrained manufacturing capacity, long vein-to-vein times, high cost of goods, and limited feasibility of deployment outside highly resourced centralized facilities. Collectively, these constraints have resulted in a mismatch between patient eligibility and actual treatment access, underscoring the need for manufacturing strategies that are scalable, cost effective, and adaptable to diverse clinical and geographic settings.

Current commercial manufacturing models are largely centralized and capital intensive, often relying on highly integrated automated systems designed to execute multiple unit operations within a single closed device [4-6]. While such systems can reduce operator variability and simplify regulatory control strategies, they also introduce practical limitations. In particular, the requirement for serial manufacturing runs using single product devices constrains throughput, limits flexibility in process development, and often underutilizes critical hardware during long culture periods. Moreover, the infrastructure, maintenance, and training requirements associated with these systems may be prohibitive for early-stage programs, academic centers, regional hospitals, and low resource environments [7-9].

An alternative approach is to use simplified, single-use manufacturing workflows in which unit operations are integrated around a common culture platform while avoiding dependence on highly automated, device-bound systems. Such workflows may retain operational flexibility by allowing individual process steps to be adapted or scheduled independently, while reducing the capital equipment, maintenance, and specialized training requirements associated with fully automated platforms. Historically, lower-resource CAR T-cell manufacturing has often relied on open or semi-closed culture vessels, including flasks and gas-permeable bags, which can introduce challenges related to scalability, sterility assurance, and labor burden. Advances in closed, single-use culture technologies have begun to address these limitations by enabling integrated GMP-compatible workflows with reduced infrastructure requirements.

The GRex® (gas permeable rapid expansion, Wilson Wolf) bioreactor platform represents one such advancement, where the defining feature is a gas permeable, liquid impermeable membrane that enables efficient oxygen transfer directly to cells while supporting a large static media reservoir. In this context, we developed a simple, closed-system, bioreactor-centered manufacturing workflow using a single-use G-Rex 100M-CS platform for GMP-compatible production of autologous CAR T cells. The workflow integrates T-cell enrichment, activation, static viral transduction, expansion, and harvest while minimizing reliance on dedicated instrumentation for individual unit operations. Here we describe the development, optimization, and at-scale demonstration of this manufacturing platform through a combination of small-scale feasibility studies and largescale proof of concept runs while evaluating process performance, product

quality, and functional potency, and discuss the implications of this approach for rightsized, phase-appropriate CAR T manufacturing across diverse clinical contexts.

Materials and Methods

Cell seeding density, activation conditions, transduction timing, and vector input were selected based on the clinically validated GD2 CAR T-cell manufacturing process used as the reference workflow for this study and were not independently optimized during initial adaptation to the G-Rex platform. Small-scale cultures were initiated using $CD4^+/CD8^+$ T cells from three healthy donors, with sufficient cells activated on Day 0 to provide 1×10^7 viable T cells per experimental condition at the time of transduction on Day 2. Cells were activated using research-grade TransAct reagent (1:100 dilution) in TexMACS medium supplemented with 3% human AB serum, 12.5 ng/mL IL-7, and 12.5 ng/mL IL-15 and were maintained at 37 °C with 5% CO_2. Retroviral transduction was performed on Day 2 using the GD2.4-1BB.CD3ζ CAR vector at a multiplicity of infection of 10, consistent with the reference clinical process. Subsequent experiments focused on optimization of G-Rex-specific process parameters, including transduction-enhancer conditions, RetroNectin coating concentration and timing, vessel retention, and media-exchange timing.
Unless otherwise described, all small-scale cultures were performed using previously enriched CD4+/CD8+ cryopreserved T cells. For the three at-scale end-to-end manufacturing runs, three leukopaks from healthy donors were used. The first leukopak was received and cryopreserved prior to enrichment and culture initiation and the second and third leukopaks were received and used fresh for enrichment and culture initiation.

Media Exchanges

For all small-scale cultures, when a media exchange was performed, approximately 85% of supernatant media was removed without disturbing the cell bed on the G-Rex plates. This volume of media corresponds to the average volume of supernatant media that can be removed from a G-Rex 100M-CS vessel when a GatheRex device is used for media exchange. For cultures that use the optimized feeding schedule, the timing of the media exchange intentionally coincides with the cell count and viability assessment to avoid adding an additional timepoint of culture disruption during the expansion phase of the manufacturing process.

Evaluation of Retroviral Transduction Enhancers

Three commonly used retroviral transduction enhancers, Protamine Sulfate (PS), Vectofusin-1 (VF), and RetroNectin (RTN), were evaluated in parallel under static and spinoculation conditions. $CD4/CD8^+$ T cells from three healthy donors were used for all experiments.

On Day 0, previously enriched cryopreserved $CD4^+/CD8^+$ T cells were thawed and activated in bulk in G-Rex 6M-well plates using research-grade TransAct, a soluble polymeric CD3/CD28 activation reagent, at a 1:100 dilution in TexMACS medium supplemented with 3% human AB serum, 12.5

ng/mL IL-7, and 12.5 ng/mL IL-15. The activation reagent, dilution, and timing were retained from the clinically validated GD2 CAR T-cell manufacturing process and were not independently optimized for the G-Rex platform. All cultures were maintained at 37 °C with 5% CO_2 until Day 2.

For RTN conditions, G-Rex 6M-well plates (static arm) or standard 6-well tissue culture plates (spinoculation arm) were coated on Day 1 with RTN at 7.2 μg/mL[2] and incubated overnight at 2-8 °C. On Day 2, excess RTN was removed, wells were washed with sterile DPBS, blocked with DPBS containing 2.5% human serum albumin (HSA), and rinsed with sterile DPBS prior to cell seeding.

For all spinoculation conditions, 1×10^7 activated cells were plated in standard 6-well tissue culture plates. For the RTN spinoculation conditions, the activated cells were plated in the previously coated, blocked and washed 6-well tissue culture plates. For the PS spinoculation conditions, activated cells were plated in 6-well tissue culture plates and PS was added directly to the cultures at a 1:1000 dilution of total culture volume to a final concentration of 10 ug/mL immediately following vector addition. For the VF spinoculation conditions, activated cells were plated in 6-well tissue culture plates and VF was diluted 1:100 in a volume of medium equal to the vector volume, mixed with the vector and added to the cell culture within 10 minutes of vector addition, per manufacturer's recommendations, to a final concentration of 10 ug/mL All spinoculation plates were centrifuged at 400 × g for 2 hours at 32 °C and then returned to the incubator until Day 3.

For all static conditions, 1×10^7 activated cells were plated in G-Rex 6M-well plates. For the RTN static conditions, the activated cells were plated in the previously coated, blocked and washed G-Rex 6M plates. For the PS static conditions, activated cells were plated in fresh G-Rex 6M-well plates and PS was added directly to the cultures at a 1:1000 dilution of total culture volume to a final concentration of 10 ug/mL immediately following vector addition. For the VF static conditions, activated cells were plated in fresh G-Rex 6M-well plates and VF was diluted 1:100 in a volume of medium equal to the vector volume, was mixed with the vector and added to the cell culture within 10 minutes of vector addition, per manufacturer's recommendations, to a final concentration of 10ug/mL. All G-Rex 6M-well plates were returned to incubator post-vector addition until Day 3.

Retroviral transduction was performed using a GD-2 CAR retroviral vector at a multiplicity of infection (MOI) of 10. All conditions were adjusted to a final transduction volume of 10 mL.

On Day 3, spinoculation cultures were transferred into fresh G-Rex 6M-well plates. All cultures were supplemented with fresh TexMACS complete media to a final volume of 100mL. Static cultures were also supplemented with fresh TexMACS complete media to a final volume of 100mL. All cultures were also supplemented with 1mL of 1mM Dasatinib solution to a final concentration of 1uM. All cultures were maintained at 37 °C with 5% CO_2.

On Day 6, from each culture, 85% of the supernatant media was removed and all cultures were supplemented with fresh TexMACS complete media to a final volume of 100mL with the addition of 1mL of 1mM Dasatinib solution to a final concentration of 1uM and maintained at 37 °C with 5% CO_2.

On Day 7, transduction efficiency was assessed by flow cytometry using a CytoFLEX LX instrument. Cell expansion and viability were recorded as secondary endpoints.

Optimization of RetroNectin Coating Density

RTN coating density was optimized in G-Rex 6-well plates (10 cm^2 growth area). Two experimental arms were evaluated: activation in RetroNectin-coated wells (Day -1 coating, Day 2 exposure) and activation in uncoated wells followed by transfer to RTN-coated wells prior to transduction (Day 1 coating, Day 2 exposure). RTN coating densities ranged from 4 to 25 µg/mL.

RTN coating solutions were prepared fresh by diluting a 1 mg/mL RTN stock in DPBS, and plates were coated and incubated overnight at 2-8 °C.

For Day -1 coating, wells were washed with DPBS, blocked with DPBS containing 2.5% HSA for 30 minutes, and rinsed prior to cell seeding on Day 0. $CD4/CD8^+$ T cells (1×10^7 per condition) from three healthy donors were plated directly into coated wells and activated with TransAct (1:100 dilution).

For Day 1 coating conditions, cells were activated in uncoated G-Rex plates on Day 0 and On Day 2, cells were transferred into RTN-coated wells prior to transduction.

All conditions were transduced on Day 2 with GD-2 CAR retroviral vector at an MOI of 10 in a final volume of 10 mL. Cultures were fed on Day 3 to a final volume of 35 mL and maintained until Day 7. Expansion, viability, and transduction efficiency were assessed on Day 7.

Effect of RetroNectin Blocking and Plate Retention

To evaluate the necessity of RTN blocking and the impact of prolonged culture in RTN-coated vessels, a two-factor experimental design was implemented: blocked versus unblocked RTN surfaces, and retention versus transfer from RTN-coated plates post-transduction.

$CD4/CD8^+$ T cells from three healthy donors were bulk activated such that 1×10^7 cells were available per condition on Day 2. On Day 1, two G-Rex 6-well plates were coated with RTN at 7.2 µg/mL and incubated overnight. On Day 2, RTN was removed and all wells were washed with DPBS. Half of the wells were blocked with DPBS containing 2.5% HSA for 30 minutes at room temperature; the remaining wells were left unblocked.

Each condition was seeded with 1×10^7 activated T cells and transduced with GD-2 CAR retroviral vector at an MOI of 10 in a final volume of 10 mL. Cultures were incubated until Day 3. On Day 3, cultures assigned to the transfer arm were moved into fresh, uncoated G-Rex plates and expanded to 35 mL. Retain arm cultures remained in the original RTN-coated wells and were similarly fed.

All cultures were maintained until Day 7 and analyzed for cell density, viability, and transduction efficiency by flow cytometry.

Optimization of Feeding Schedule in G-Rex Culture

Feeding strategies were optimized using two seeding densities (1×10^7 or 2×10^7 cells) across five feeding conditions per arm. Cultures were initiated in G-Rex 6M plates using research-grade TransAct at a 1:100 dilution in 7 mL of medium.

Feeding regimens included feeding on Day 2 or Day 3 post-activation, with or without media exchange on Day 6. These conditions were compared to a clinical reference process consisting of feeding on Day 3, media exchange on Day 5, and harvest on Day 7. Duplicate cultures from three donors were evaluated.

Longitudinal Phenotypic Characterization During Culture

To assess phenotypic evolution during culture, seven identical culture plates were initiated using CD4/CD8$^+$ T cells from three donors seeded in duplicate at 1×10^7 cells per condition. Cultures were activated with research-grade TransAct at a 1:100 dilution in 7 mL of medium.

At each time point (Days 2-7), one replicate culture was harvested for flow cytometric analysis of activation (4-1BB, CD69, HLA-DR, CD25), memory (CD45RA, CD45RO, CCR7, CD62L, CD95), and exhaustion (TIM-3, LAG-3, PD-1, CD39) markers, along with expansion and viability measurements. Remaining cells were cryopreserved in Plasmalyte supplemented with 4% HSA and CryoStor CS10 and stored at -160 °C. For memory populations the gating strategy applied was as follows: Lymphocytes > Single Cells > Viable Cells > CD3+ Cells > CD4+ / CD8+ cells. Subsequently we analyzed CD4+ or CD8+ subsets as follows: CD4+/CD8+ > CAR+ cells > CCR7+ / CD45RA+; Central memory cells: CCR7+CD45RA-; Effector memory cells: CCR7-CD45RA-; Terminally differentiated effector memory cells: CCR7-CD45RA+; Naive memory cells: CCR7+CD45RA+

The paired replicate culture was maintained according to a standardized clinical process (transduction on Day 2, feeding on Day 3, media exchange on Day 6, harvest on Day 7). Cryopreserved samples were later thawed and co-cultured with GD2 expressing tumor cell lines. GD2-expressing tumor target cell lines used for functional testing included NALM-6, a human B-cell acute lymphoblastic leukemia cell line engineered to express GD2; SY5Y, a human neuroblastoma cell line; 143B, a human osteosarcoma cell line; and MG63.3, a GD2-expressing derivative of the human osteosarcoma cell line MG63. These target cell lines were used to evaluate CAR T cell cytokine secretion and cytotoxic activity across hematologic and solid tumor models. Cytokine secretion (IL-2 and IFN-γ) was quantified from supernatants using ELISA.

SepaRex-Based Enrichment and End-to-End Large-Scale Manufacturing

A novel SepaRex magnetic enrichment workflow was developed for large-scale CD4/CD8$^+$ T-cell isolation from leukapheresis material. Leukopaks from three healthy donors were processed using detachable CD4 and CD8 Dynabeads at a bead-to-target ratio of 4:1. Target cell frequencies were determined by flow cytometry prior to processing, and leukopak volumes were adjusted to achieve post-wash target cell concentrations $>1 \times 10^7$ cells/mL.

Processing was performed in a G-Rex 100M-CS vessel equipped with a closed, multi-line fluid-transfer set and positioned on a SepaRex magnetic base. Initially, CD4 and CD8 detachable beads (CTS™ Detachable Dynabeads™, Thermo) were added in the vessel and washed using 100mL of DPBS supplemented with 1% HSA. The vessel was placed on the magnetic base and allowed for 5' capture time after which the supernatant wash volume was removed from the vessel. Leukapheresis material was then added directly in the vessel with detachable CD4 and CD8 magnetic beads at a bead-to-target-cell ratio of 4:1 and mixed to support binding to target cells for a total of 30 minutes of binding time while rocking on a platform rocker (-15^{o} to +15^{o} tilt per 30 seconds). Following this positive selection step, the vessel was removed from the platform rocker and placed on the magnetic base, and the magnetic field was applied to immobilize bead-bound $CD4^{+}$ and $CD8^{+}$ T cells against the gas-permeable membrane surface for a total of 10 minutes capture time. The supernatant containing non-target cells was then removed through the closed fluid-transfer set utilizing the GatheRex device. The magnetic field was subsequently removed, and a release (dissociation) buffer (CTS™ Detachable Dynabeads™ release buffer, Thermo) was added to detach the beads from the target cells for a total of 60 minutes of release time while rocking on a platform rocker (-15^{o} to +15^{o} tilt per 30 seconds). The vessel was then returned to the magnetic base for 10 minutes to capture the released beads, allowing the bead-free enriched $CD4^{+}$/$CD8^{+}$ T cells in suspension to be transferred to a target cell collection bag within the closed system. Following the same process as above, two washes of the vessel were performed using 100mL of TexMACS complete media each time to increase target cell recovery. The harvested cells were used for enumeration and flow-cytometric characterization. Following target cell isolation, enriched T cells were collected and confirmed by flow cytometry (CD3, CD4, CD8, TBNK markers).

Immediately following enrichment, 1×10^{8} viable $CD4^{+}$/$CD8^{+}$ T cells were seeded into a RetroNectin-coated G-Rex 100M-CS vessel, corresponding to approximately 1×10^{6} cells/cm^{2} of gas-permeable growth surface, and activated using research-grade TransAct at the manufacturer-recommended dilution (1:100). The activation cell input, Day 2 transduction timing, and retroviral vector input of MOI 10 were retained from the clinically validated GD2 CAR T-cell reference process rather than independently re-optimized for the manufacturing-scale G-Rex workflow. On Day 2, cultures were transduced with the GD2.4-1BB.CD3ζ CAR retroviral vector at an MOI of 10. and a final transduction volume of 100mL. On Day 3, cultures were brought to a final volume of 1 L, the maximum working culture volume used in the G-Rex 100M-CS process. This volume was selected to support nutrient availability through the remaining culture period while minimizing repeated culture manipulation. Media exchange was performed on Day 6 utilizing the GatheRex device by removing 80-85% of the culture supernatant, and cultures were subsequently harvested on Day 7.

Final products were analyzed for phenotype, cryopreserved, and later evaluated in co-culture assays with GD-2 expressing tumor lines using ELISA-based cytokine measurements and IncuCyte-based cytotoxicity assays at effector-to-target ratios of 1:1, 1:5, and 1:10.

Dasatinib addition

Unless otherwise mentioned, dasatinib solution is added to the cultures on Day 3 and Day 6. Depending on the vessel used (G-Rex 6M-plates or G-REX 100M-CS vessels), stock dasatinib solution (1mM) is diluted 1:100 in the final culture volume to achieve a concentration of 1uM.

Cell enumeration and Viability assessment

For all cell counting and viability measurements, we used a Cellometer Auto 2000 cell viability counter (Revvity Inc.) or a Cellaca MX cell counter (Revvity Inc.) using ViaStain™ AOPI staining solution (Revvity Inc.). We utilized the appropriate counting protocol on each device based on manufacturer's recommendations and the cell type (apheresis-high RBC, cultured T cells-low RBC).

DynaCellect enrichment

The DynaCellect is an automated closed system enrichment device (Thermo) utilizing a single-use tubing set to transfer volumes of beads, washing and release buffers, apheresis material and enriched target cells to and from a rocking separation chamber that employs a retractable plate magnet to immobilize magnetic separation beads. The protocol utilized for enrichment of CD4+/CD8+ T cells starts by transferring predetermined volumes of CD4 and CD8 releasable beads (CTS™ Detachable Dynabeads™, Thermo) in the separation chamber along with DPBS/1% HSA solution to wash the magnetic beads by immobilizing the beads with the use of the plate magnet and removing the wash buffer along with the preservative solution the beads are shipped in. This is followed by addition of the apheresis material at a 4:1 bead to target cell ratio and a 30 minute incubation time with a continuous –30^{o} to +30^{o} tilt rocking motion per minute to ensure adequate mixing of target cells and magnetic beads. After this capture time, the plate magnet is engaged for 2 minutes and immobilizes the bead-bound CD4+ and CD8+ T cells. The supernatant containing non-target cells is transferred to a waste bag in the closed-system tubing. Subsequently, the magnetic plate is disengaged and 100mL of release buffer (CTS™ Detachable Dynabeads™ release buffer, Thermo) is added in the separation chamber to release the magnetic beads from the target cells followed by a 60 minute incubation time with a continuous –30^{o} to +30^{o} tilt rocking motion per minute to ensure adequate mixing. After this release time, the plate magnet is engaged for 2 minutes and immobilizes the magnetic beads leaving the CD4+/CD8+ target cells in suspension. The cell suspension is transferred to a target cell collection bag. This protocol utilizes two bead washing cycles using complete media. For each cycle, 100mL of TexMACS complete media is transferred in the separation chamber, the plate magnet is disengaged and a rocking motion is utilized to mix the beads and increase target cell recovery. The plate magnet is engaged for 2 minutes and the wash volume is also transferred to the target cell bag. At the end of the process, the cells in the target cell bag are used for enumeration, viability measurement, enrichment efficiency and target cell purity and downstream processing for CAR T cell culture initiation.

Tumor cells antigen expression quantification

The tumor lines, each co-expressing a GFP protein, were used for the co-cultures and killing assays, were cultured, passaged and expanded in tissue culture flasks using RPMI-1640 (ATCC modification) media (Thermo Scientific) supplemented with 10% heat inactivated and gamma irradiated fetal bovine serum (Thermo Scientific). On the day of co-culture setup, samples from each tumor line were used to assess for GD2 antigen expression. 1 x 10^6 tumor cells from each tumor line were stained in triplicate with PE anti-human Ganglioside GD2 antibody (Biolegend) and were then assessed by flow cytometry on the Cytoflex LX instrument. In parallel, beads from a BD Quantibrite™ PE Phycoerythrin Fluorescence Quantitation Kit were used on the Cytoflex LX to generate a standard curve according to manufacturer's recommendations and bead lot specifications. The observed geometric mean values for the positive peaks of the stained tumor cells were used to calculate molecules per cell for each tumor line according to the standard curve. The GD2 antigen expression for each tumor line is outlined in supplementary figure 6.

Results

Development of a G-Rex-Based Manufacturing Framework Modeled on a Clinically Validated Process

To establish a foundation for a closed, scalable manufacturing platform, we utilized GD2directed CAR T cells as a model, enabling direct comparison to historical products manufactured using a CliniMACS Prodigy-based process for a first-in-human clinical trial targeting diffuse intrinsic pontine glioma (DIPG) and spinal diffuse midline glioma (sDMG) (NCT04196413) [10, 27]. (Figure 1a). In the CliniMACS Prodigy-based workflow, autologous T cells are enriched from apheresis on Day 0 and activated using TransAct according to the manufacturer's dose recommendation. On Day 2, cells are transduced in the presence of a transduction enhancer using a retroviral vector encoding the GD2.4-1BB.CD3ζ chimeric antigen receptor (CAR) with the aid of spinoculation. Cells are cultured in TexMACS medium supplemented with IL-7 and IL-15 cytokines and expanded in the presence of dasatinib, a reversible tyrosine kinase inhibitor shown to suppress CAR-mediated tonic signaling and prevent premature T-cell activation during ex vivo expansion [14]. Cells are cryopreserved on Day 7 of culture. We began by adapting and optimizing key elements of this protocol at small-scale using G-Rex 6M well plates, focusing on viral vector transduction parameters, culture conditions, and capture of analytics across each culture day. Following bench-scale optimization, the process was translated to manufacturing scale by integrating a novel in-vessel enrichment strategy with activation, static transduction, expansion, and harvest in a G-Rex 100M-CS-centered workflow.

Small-Scale Optimization of Viral Vector Transduction in a G-Rex Static Bioreactor

Transduction enhancers such as Vectofusin-1 (VF), protamine sulfate (PS), and Retronectin (RTN) are widely used to improve viral gene transfer in both retroviral and lentiviral systems [15-17], particularly when combined with spinoculation, which facilitates close contact between viral particles and target T cells. However, the commercially available G-Rex bioreactor is not amenable to traditional spinoculation. To provide a pathway for effective use of transduction enhancers, we explored the use of RTN coating on the gas permeable membrane of the G-Rex vessel. To establish

effective conditions for retroviral transduction within the G-Rex platform, we performed a series of small-scale optimization studies focused on Day 2 of culture, aligning with the standard timing of transduction in the clinical protocol. These studies were designed to determine optimal parameters for maximizing transduction efficiency while maintaining T cell viability, phenotype, and expansion kinetics. Initial experiments were conducted in the G-Rex6M format using activated T cells prepared under closed-system conditions. Cells were activated on Day 0 and cultured in medium supplemented with IL-7 and IL-15 (12.5 ng/mL each) and 1 µM dasatinib (see methods), as previously described. On Day 2, cells were transduced with a retroviral vector encoding the GD2.4-1BB.CD3ζ CAR-iCasp9 construct under varying conditions.

Initial studies demonstrated that the G-Rex surface could be successfully coated with RTN, and that this coating significantly improved transduction efficiency under static culture conditions. Specifically, the decrease in transduction efficiency observed in non-spinoculated cultures using other enhancers was recovered with RTN coating, resulting in comparable transduction efficiency between the clinical VectoFusin/spinoculation condition and the static RTN coated condition (Figure 1b). Importantly, fold expansion was not significantly different across conditions using VectoFusin, protamine sulfate, or RTN as transduction enhancers. However, because transduction efficiency was highest in the static RTN condition, this condition generated the greatest total CAR+ cell yield (Figure 1c). Cells transduced under static conditions exhibited a trend toward improved expansion compared to those transduced using spinoculation-based methods, while viability remained unaffected across all conditions (Supplementary Figure 1). These findings are significant as they suggest RTN coating can serve as a viable alternative to spinoculation-based enhancement methods, enabling efficient transduction of both retroviral and lentiviral vectors in the G-Rex static bioreactor system.

To further optimize static transduction in the G-Rex format, we investigated two key process variables: (1) the optimal surface density of RTN coating and (2) the feasibility of initating culture in a pre-coated vessel versus using a freshly coated G-Rex on Day 2. Streamlining the process by reducing vessel manipulations and consolidating processing steps can minimize cell losses and lower the risk of contamination, while also decreasing material usage, hands-on time, and overall manufacturing costs. We performed a titration of RTN coating density ranging from 4 to 25 µg/mL and assessed its impact on transduction efficiency (TE), total CAR+ cell output, and overall fold expansion by Day 7. Across multiple donors, we did not observe any significant differences in these parameters across the RTN coating densities evaluated; therefore, we proceeded with 7.2 µg/mL for subsequent small- and large-scale experiments. To assess the timing of RTN application, we compared transduction outcomes in fresh vessels coated on Day 1 immediately prior to transduction versus those pre-coated on Day -1 prior to T cell activation and maintained throughout the 48-hour stimulation period. While TE was modestly higher in the Day 2 coating condition, we found that RTN-coated surfaces prepared on Day -1 retained sufficient functional activity to support >40% transduction efficiency and >10-fold expansion by Day 7 (Figure 1d). These findings supported a streamlined workflow in which the G-Rex vessel is coated with RTN on Day -1, enabling a closed, continuous workflow from T cell activation through transduction without a vessel transfer. Finally, based on prior reports suggesting that RTN-coated surfaces may require pre-blocking with serum albumin to prevent non-specific interactions that impair transduction

efficiency, we evaluated whether blocking the coated G-Rex surface was necessary in our system. This practice is commonly recommended in commercial protocols for RTN use [18], and has been described in large-scale retroviral transduction methods to reduce non-specific adsorption of viral particles and cellular debris [19]. We observed no significant differences in transduction efficiency, CAR+ cell yield, or expansion when RTN-coated vessels were blocked versus unblocked (Supplementary Figure 2), supporting the omission of blocking from our optimized process.

Evaluation of Media Replenishment Timing and Its Impact on Cell Expansion in G-Rex Cultures

The G-Rex platform is designed to support static, unperturbed expansion with minimal manipulation, provided that cell density and nutrient demands remain within the operational capacity of the bioreactor. Periodic sampling and media replenishment may be necessary during manufacturing to support decision-making for harvest timing and quality assurance. To assess the impact of media exchange timing on cell expansion and viability, we modeled a 7-day culture protocol based on the clinical GD2 CAR T cell workflow and evaluated growth kinetics following various post-transduction media exchange intervals. Specifically, G-Rex cultures were seeded with 100 million activated T cells ($1x10^6$ cells/cm^2) and transduced on Day 2. Cultures were either left undisturbed or subjected to a single media exchange at 24-, 48-, 72-, 96- or 120-hours post-transduction. Fold expansion and viability were assessed on harvest (Day 7). Results demonstrated that media exchange at any time point within the 24–96-hour window post-transduction had no significant impact on final cell yield or viability compared to undisturbed cultures (Figures 1e and 1f). Although the media exchange performed at 120 hours post-transduction, corresponding to the Day 5-7 interval, showed a trend toward reduced expansion in two of three donors, this difference was not statistically significant. Because media exchange required resuspension and disruption of cells from the gas-permeable membrane surface, these findings supported limiting unnecessary late-stage manipulation. The manufacturing-scale workflow therefore used a final culture volume of 1 L and a single planned media exchange to support nutrient availability while minimizing process interventions. All conditions supported similar fold expansion trajectories, indicating that G-Rex-based cultures maintain robust performance without requiring tightly scheduled feeding interventions. These findings reinforce the suitability of the platform for simplified manufacturing workflows, particularly in settings where continuous process monitoring or automation is not available.

Characterization of T Cell Phenotype and Function During G-Rex Culture on RTN-Coated Surfaces

Using the selected G-Rex process conditions established through the optimization studies described, including RTN-mediated static transduction and the selected media-management strategy, we longitudinally characterized CAR T-cell phenotype and function across the 7-day culture period. Consistent with prior studies describing activation of T cells through CD3/CD28 stimulation, we observed a transient upregulation of immune checkpoint molecules PD-1, LAG-3, and TIM-3 (Figures 2a, b) in both CD4 and CD8 populations, known to act as a negative feedback mechanism to restrain overactivation and limit immune-mediated damage [20,21]. In parallel, we observed a gradual increase in CD39 expression beginning approximately 72 hours post-activation (Day 4), a feature associated with prolonged ex vivo culture and sustained T cell stimulation [22].

Elevated CD39 expression has been linked to functional impairment, including reduced cytokine production and diminished cytotoxicity against tumor targets [23], and with poorer clinical outcomes in adoptive cell therapy settings, underscoring its relevance as a manufacturing biomarker [24]. Consistent with these findings, our cytotoxicity assays demonstrated faster killing kinetics when cultures were harvested prior to Day 4 (Supplementary Figure 3, Figure 2i). Activation also induced the expected increase in T cell activation markers, 4-1BB, CD69, and CD25, with a progressive tapering of HLA-DR expression as naïve T cells differentiated over the culture period (Figures 2c, d). Phenotypic analysis revealed that the T cell population achieved a maximal central memory (T_{CM}) phenotype (*CD45RO+, CCR7+*) by Day 4 of culture (Figures 2e, f), along with rapid upregulation of effector molecules IL-2 and IFN-γ (Figures 2g, h), tapering off by Day 7.

Fully-closed, At-Scale End-to-End CAR-T Manufacturing Workflow in G-Rex

To enable a simplified, cost-effective, and fully integrated CAR T cell manufacturing process within the G-Rex platform, we developed a novel strategy for performing $CD4^+/CD8^+$ T cell enrichment directly within the G-Rex100M-CS bioreactor (Figure 3a). In this approach, donor apheresis material is combined with detachable CD4/CD8 beads (Thermo) inside the G-Rex100M-CS, which is secured on a SepaRex magnetic base plate (Wilson Wolf Manufacturing) that enables selective capture and release of target cells. Upon application of a magnetic field, $CD4^+$ and $CD8^+$ T cells bound to beads are immobilized on the membrane surface, and non-target cells are removed through a gentle wash. The vessel is removed from the magnetic base plate to allow resuspension of the bead-bound target cells into a dissociation buffer (ThermoFisher), enabling bead detachment. The vessel is reintroduced to the magnetic field to clear residual beads to the membrane floor, and the bead-free enriched CD4+/CD8+ T cells are transferred to a collection bag for enumeration and phenotypic assessment. This method is adaptable to various bead formats and sizes and can be modified to enrich bead-negative populations in cases where depletion strategies are desired.

To evaluate the feasibility and efficiency of this in-G-Rex enrichment method, we performed $CD4^+/CD8^+$ selection on apheresis material from three healthy donors using the workflow described above. The average recovery of enriched T cells was 61.6% ± 8.6%, and the purity of $CD4^+$ and $CD8^+$ T cells in the post-selection product was 87.2% ± 7.9% and the CD4:CD8 ratio was not majorly impacted pre- and post-enrichment (Figure 3b, c, d). To contextualize these results, we compared the recovery and purity outcomes from our G-Rex–based enrichment strategy with datasets generated using alternative GMP-compatible enrichment platforms, including CliniMACS Prodigy and Dynacellect systems used across active clinical trials and development studies conducted in our lab (Table 1). Overall, our simplified in-vessel approach yielded enrichment performance metrics that were comparable to or better than those achieved using industry-gold-standard GMP platforms. A detailed compositional breakdown of immune phenotypes at each stage of enrichment is provided in Supplementary Figure 4. Enriched $CD4^+/CD8^+$ T cell populations were seeded into individual G-Rex100M-CS vessels that had been pre-coated with RTN on Day -1. Following seeding, cells underwent activation using research-grade TransAct at a 1:100 dilution and placed in incubator for 48 hours. Cultures were transduced on Day 2, using a GD2-directed CAR retroviral vector (MOI = 10). 24 hours after transduction, cultures were supplemented with

fresh TexMACS complete media to a final volume of 1L with the addition of Dasatinib solution to a final concentration of 1uM. On Day 6, supernatant media was removed using the GatheRex device resulting in a 80-85% volume reduction. All cultures were subsequently supplemented with fresh TexMACS complete media to a final volume of 1L with the addition of Dasatinib solution to a final concentration of 1uM until Day 7. Cultures were harvested on Day 7, consistent with the minimal manipulation and single-media-feed strategy indicated by our small-scale optimization studies. The average CAR transduction efficiency achieved was 62.3% ± 5.1%, with a fold-expansion of 26.8 ± 4.7 at harvest. Final product purity remained high, with >96% $CD3^+$ T cells, and cell viability exceeded 94% ± 3.2%, indicating robust downstream expansion and minimal contamination with non-T cells. Products generated using the 1-L culture workflow retained a predominantly central memory phenotype with low expression of exhaustion-associated markers, consistent with the profiles observed in the small-scale Day 6 media-exchange condition.

To benchmark the at-scale end-to-end G-Rex manufacturing workflow, we compared key manufacturing performance metrics with historical data from the Prodigy-based GD2-CAR T cell clinical trial (NCT04196413) (Figures 3d-i, Table 2). The G-Rex-based approach demonstrated comparable transduction efficiencies, expansion potential, and final product functional quality, while maintaining high viability and a favorable central memory phenotype. At harvest, expression of CD39, LAG-3, and TIM-3 was comparable between G-Rex and Prodigy-manufactured products, whereas PD-1 expression was significantly lower in the G-Rex condition. This pattern suggests that the G-Rex workflow did not broadly increase exhaustion-associated marker expression and may be associated with a selectively lower PD-1 phenotype at harvest.

Functional assessments, including cytokine secretion and tumor-cell killing assays, closely mirrored results from small-scale studies, supporting the scalability and predictive power of the optimized workflow from $10cm^2$ to $100cm^2$ reactor sizes. Notably, this scale-down model for development work is difficult to achieve when using highly automated systems that lack a miniaturized format of their full process. Collectively, these findings demonstrate that a simplified, closed-system G-Rex process can achieve clinically relevant outcomes while minimizing infrastructure demands, enabling broader deployment across academic and decentralized manufacturing settings.

Discussion

The rapid expansion of CAR T cell therapies has intensified the need for manufacturing platforms that can balance product quality, operational flexibility, and economic sustainability. In this study, we describe a closed, bioreactor-centered manufacturing workflow that integrates key unit operations, including T-cell enrichment, activation, transduction, expansion, and harvest, while maintaining clinically relevant product attributes. By grounding development in a clinically validated GD2 CAR T-cell process and benchmarking against historical trial data, we demonstrate that this lower-resource approach can achieve comparable manufacturing performance without reliance on highly automated, device-bound systems. This establishes space to innovate manufacturing methodology without compromising clinically relevant product quality attributes.

A central feature of this workflow is its operational simplicity and flexibility. Although multiple unit operations are performed within or around a common G-Rex platform, individual process steps can be adapted without requiring redesign of a fully automated, fixed-sequence system. Efficient static viral transduction using RTN-coated G-Rex membranes eliminates the need for spinoculation and associated centrifugation equipment, thereby reducing capital requirements and process complexity. A key innovation of this study is the development of a closed workflow for direct magnetic $CD4^+/CD8^+$ enrichment within the G-Rex vessel, eliminating the need for a separate cell-selection instrument. Together, these features reduce hands-on complexity, simplify training, and preserve the ability to scale manufacturing capacity incrementally. A comparative cost analysis demonstrates the significant upfront infrastructure investment required to establish GMP manufacturing capabilities using automated systems versus the G-Rex-based approach (Table 3).

Importantly, phenotypic and functional analyses across culture time points revealed predictable activation, memory differentiation, and exhaustion marker dynamics consistent with prior reports in CAR T manufacturing. The lower PD-1 expression observed in G-Rex-manufactured products should be interpreted cautiously, as PD-1 can reflect both activation history and exhaustion state, and CD39, LAG-3, and TIM-3 were comparable between platforms. However, this finding is consistent with prior evidence that manufacturing platforms can influence CAR T phenotype and exhaustion-related programs. The static, gas-permeable G-Rex format supports oxygenation and nutrient availability without routine stirring, rocking, or perfusion, whereas automated workflows involve intermittent mixing and fluid handling. Thus, differences in mechanical exposure, oxygenation, cell density, or media exchange dynamics may contribute to the observed platform-specific difference in PD-1 expression [30, 31]. Additional studies would be needed to define the underlying mechanism. The temporal dependence of markers such as CD39 highlights the value of longitudinal phenotypic monitoring for informing harvest timing and underscores how simplified platforms can still support data-driven process decisions. The concordance between small scale and at-scale results further supports the use of linearly scalable GRex formats as effective development models, enabling iterative optimization without committing early to large, fixed-capacity manufacturing infrastructure.

This study provides a foundation for developing CAR T-cell manufacturing workflows using the end-to-end G-Rex workflow. Although G-Rex-based and automated-manufactured products demonstrated similar manufacturing performance and *in vitro* function, the study was not designed to establish formal comparability. If an established clinical process were transitioned to a G-Rex workflow, matched donor material should be split and manufactured in parallel to compare process performance metrics and additional characterization, including proliferative capacity, molecular profiling, or in vivo activity, may be warranted because platform-specific differences in culture conditions may impact product phenotype, persistence, or efficacy.

The scope of this study focused on formal process optimization using a single GD2 retroviral vector. We have subsequently applied the broader G-Rex workflow to additional CAR constructs using both retroviral and lentiviral vectors, as well as to nonviral CRISPR-based editing approaches, while retaining core parameters such as activation, seeding density, culture volume, feeding schedule, and harvest timing. Nevertheless, vector- and construct-specific transduction or editing

performance should be confirmed, with adjustment of vector input, MOI, transduction-enhancer strategy, coating conditions, or editing parameters as needed.

Beyond enabling efficient translation from bench-scale studies to manufacturing-scale execution, the linear scalability of the GRex platform also supports the converse: the establishment of scientifically justified reduced scale models derived directly from the commercial process. Regulatory authorities have increasingly emphasized the value of such models for developing process understanding and control strategies [32,33]. Notably, the European Medicines Agency has described the use of a "Qualified Reduced Scale Model" as a mechanism to establish Proven Acceptable Ranges, perform expansive one-factor-at-a-time studies, and implement design of experiments without undue reliance on full-scale manufacturing runs, as described in the Public Assessment Report for CARVYKTI [34]. The availability of linearly scalable GRex formats, spanning well-plate scale through manufacturing scale bioreactors, provides a practical and predictive framework for qualifying such reduced scale models. This bidirectional scalability enables robust process characterization, lifecycle optimization, and postapproval change management while minimizing material consumption, operational burden, and risk to clinical supply.

From an operational perspective, this platform is particularly well suited for high-throughput manufacturing scenarios typical of academic cancer centers with a robust pipeline of early-phase clinical trials, investigator-initiated trials, and rare disease programs. In these contexts, the flexibility to scale capacity incrementally, adapt workflows to evolving constructs, and minimize upfront capital investment is often more impactful than maximal automation. Moreover, the operational flexibility of the integrated G-Rex process reduces constraints inherent to fully automated, fixed-capacity systems, particularly the limitation imposed by serial manufacturing on a single instrument. Parallel processing for high-throughput, large production volume scenarios simply requires additional incubators.

Decentralized and distributed manufacturing models minimizes reliance on centralized facilities, reducing turnaround times and allowing broader patient access, especially critical for rare diseases, low-resource settings, and investigator-initiated trials [25,26, 28, 29]. The simplicity and compact footprint of the G-Rex based workflow described here make it amenable to implementation in academic GMP facilities, regional hospitals, and other settings where extensive automation infrastructure may not be feasible.

Conclusion

This study establishes a closed, G-Rex-centered CAR T-cell manufacturing workflow that integrates T-cell enrichment, activation, static viral transduction and expansion within a scalable bioreactor platform. By enabling $CD4^+/CD8^+$ enrichment directly in the G-Rex and eliminating the need for separate enrichment instrumentation or spinoculation hardware, this approach reduces process complexity while preserving clinically relevant product attributes. The linear scalability of the G-Rex platform further supports both efficient translation from bench-scale optimization to manufacturing-scale production and the development of representative reduced-scale models for future process characterization. Together, these features provide a practical framework for phase-

appropriate, cost-conscious CAR T-cell manufacturing that can be adapted to academic GMP facilities, decentralized production models and high-throughput centralized manufacturing programs. Future studies across additional constructs, vector systems and cell therapy modalities will help define the broader applicability of this platform.

Declaration of competing interest

Competing Interests: C.L.M. holds equity in Link Cell Therapies and Ensoma, which are developing CAR-based therapies; consults for Link, Immatics, Ensoma, Astra-Zeneca, Moderna, Kite Pharma, Grace Science and Red Tree Capital. Dan Welch, John Wilson, and Dan Fick are employees of Wilson Wolf Manufacturing, and Andrew Scheffler is an employee of ScaleReady. The remaining authors declare no competing interests.

Funding

This work was supported by NIH Grants: R01CA263500, R35CA283888, 2P30CA124435-16, the California Institute for Regenerative Medicine (CLIN2-12595), the Virginia and D.K. Ludwig Fund for Cancer Research, CureSearch, and.the Parker Institute for Cancer Immunotherapy. C.L.M. is a Member of the Parker Institute for Cancer Immunotherapy, which supports the Stanford University Cancer Immunotherapy Program and a Weill West Coast Cancer Hub Investigator. This work was supported in part by funding and in-kind support from Wilson Wolf Manufacturing/ScaleReady through the Scale Ready Grant Program, Grant Code: 00000103.

Author Contributions

N.G-L, A.R., R.H.T. designed the experiments. N.G-L, A.R., performed the experiments and analyzed the data. R.H.T wrote the manuscript. All authors reviewed and edited the manuscript., R.H.T., S.A.F, C.L.M supervised all aspects of the work.

Acknowledgements

The authors acknowledge Dan Welch, John Wilson, and Dan Fick of Wilson Wolf Manufacturing for designing the SepaRex magnet devices used in this work. We also thank Andrew Scheffler of ScaleReady for interpretation of the broader impact of this work.

Trademark Acknowledgements

References

1. June CH, Sadelain M. Chimeric Antigen Receptor Therapy. N Engl J Med. 2018;379(1):64–73.
2. Fesnak AD, June CH, Levine BL. Engineered T cells: the promise and challenges of cancer immunotherapy. Nat Rev Cancer. 2016;16(9):566–581.

3. Labanieh L, Majzner RG, Mackall CL. Programming CAR-T cells to kill cancer. Nat Rev Immunol. 2022;22(3):155–166.
4. Levine BL, Miskin J, Wonnacott K, Keir C. Global manufacturing of CAR T cell therapy. Mol Ther Methods Clin Dev. 2017;4:92–101.
5. Kaiser AD, Assenmacher M, Schroeder T, et al. Towards a commercial process for the manufacture of genetically modified T cells for therapy. Cancer Gene Ther. 2015;22(2):72–78.
6. Hartmann J, Schüßler-Lenz M, Bondanza A, Buchholz CJ. Clinical development of CAR T cells—challenges and opportunities in translating innovative treatment concepts. EMBO Mol Med. 2017;9(9):1183–1197.
7. Abou-El-Enein M, Bauer G, Reinke P. The Business Case for Cell and Gene Therapies. Nat Biotechnol. 2021;39(9):1051–1055.
8. Hossain N, Heslop HE, Li L. Manufacturing challenges and current cell and gene therapy production strategies for viral vector and CAR T cell products. Curr Opin Biomed Eng. 2022;21:100362.
9. Marin Navarro S, Bonini C, Vermeulen M, et al. Expanding access to CAR T cell therapies through local manufacturing. Nat Rev Bioeng. 2023;1:344–358. https://doi.org/10.1038/s41587-023-01981-8
10. Majzner RG, Theruvath JL, Nellan A, et al. GD2-directed CAR T cells for neuroblastoma: a phase 1 clinical trial. Nat Med. 2022;28(6):1183–1190. https://doi.org/10.1038/s41591-021-01633-4
11. Bonifant CL, Jackson HJ, Brentjens RJ, Curran KJ. Toxicity and management in CAR T-cell therapy. Mol Ther Oncolytics. 2016;3:16011.
12. Marks P, Gottlieb S. Balancing Safety and Innovation for Cell-Based Regenerative Medicine. N Engl J Med. 2018;378(10):954–959.
13. Majzner RG, Theruvath JL, Nellan A, et al. GD2-directed CAR T cells for neuroblastoma: a phase 1 clinical trial. Nat Med. 2022;28(6):1183–1190.
14. Weber EW, Parker KR, Sotillo E, et al. Transient rest restores functionality in exhausted CAR-T cells through epigenetic remodeling. Science. 2019;365(6454):162–168.
15. Fenard D, Ingrao D, Seye A, Buisset J, Genries S, Martin S, Kichler A, Galy A. Vectofusin-1, a new viral entry enhancer, strongly promotes lentiviral transduction of human hematopoietic stem cells. Mol Ther Nucleic Acids. 2013 May 7;2(5):e90. doi: 10.1038/mtna.2013.17. PMID: 23653154; PMCID: PMC4817938.
16. Cornetta K, Duffy L, Turtle CJ, Jensen M, Forman S, Binder-Scholl G, Fry T, Chew A, Maloney DG, June CH. Absence of Replication-Competent Lentivirus in the Clinic: Analysis of Infused T Cell Products. Mol Ther. 2018 Jan 3;26(1):280-288. doi: 10.1016/j.ymthe.2017.09.008. Epub 2017 Sep 12. PMID: 28970045; PMCID: PMC5762981.
17. Morita, S., T. Kojima, and T. Kitamura. "Plat-E: an efficient and stable system for transient packaging of retroviruses." Gene Therapy, vol. 7, no. 12, 2000, pp. 1063–1066. https://doi.org/10.1038/sj.gt.3301206
18. Takara Bio. *RetroNectin Reagent Protocol.* Cat. No. T100A/B. May 2017. https://www.takara.co.kr/file/manual/pdf/T100A_B_e.v1705.pdf
19. Dodo, K., et al. "An efficient large-scale retroviral transduction method involving preloading of retroviral vector into fibronectin-coated bag." *Molecular Therapy – Methods & Clinical Development*, vol. 1, 2014, p. 14015. https://doi.org/10.1371/journal.pone.0086275
20. Sabins, Nina C., et al. *Differential Expression of Immune Checkpoint Modulators on In Vitro Primed CD4⁺ and CD8⁺ T Cells.* Frontiers in Immunology, vol. 7, 2016, article 221. https://doi.org/10.3389/fimmu.2016.00221

21. Roussel, Mikaël, et al. *Functional characterization of PD1⁺TIM3⁺ tumor-infiltrating T cells in DLBCL and effects of PD1 or TIM3 blockade.* Blood Advances, vol. 5, no. 7, 2021, pp. 1816–1829. https://doi.org/10.1182/bloodadvances.2020003080
22. Canale FP, Ramello MC, Núñez N, Araujo Furlan CL, Bossio SN, Gorosito Serrán M, Tosello Boari J, Del Castillo A, Ledesma M, Sedlik C, Piaggio E, Gruppi A, Acosta Rodríguez EA, Montes CL. CD39 Expression Defines Cell Exhaustion in Tumor-Infiltrating CD8+ T Cells. Cancer Res. 2018 Jan 1;78(1):115-128. doi: 10.1158/0008-5472.CAN-16-2684. Epub 2017 Oct 24. PMID: 29066514.
23. Klysz, Dorota D., Voss, David M., et al. *Inosine induces stemness features in CAR-T cells and enhances potency.* Cancer Cell, vol. 42, no. 2, 2024, pp. 266–282.e8. https://doi.org/10.1016/j.ccell.2024.01.002
24. Zou, Fan, et al. *Moderate expression of CD39 in GPC3-CAR-T cells shows high efficacy against hepatocellular carcinoma.* Frontiers of Medicine, vol. 18, no. 4, 2024, pp. 708–720. https://doi.org/10.1007/s11684-024-1071-9
25. Levine BL, Miskin J, Wonnacott K, Keir C. *Global access to CAR T cell therapy: decentralization opportunities*. Nat Biotechnol. 2017;35(8):703–706.
26. Mock U, Nickolay L, Philip B, et al. *Academic GMP manufacturing of CAR T cells.* Front Immunol. 2020;11:1801. https://doi.org/10.3389/fimmu.2020.01801
27. Monje, M., Mahdi, J., Majzner, R. et al. Intravenous and intracranial GD2-CAR T cells for H3K27M+ diffuse midline gliomas. Nature 637, 708–715 (2025). https://doi.org/10.1038/s41586-024-08171-9
28. Mackall, C.L., Bollard, C.M., Goodman, N. et al. Enhancing pediatric access to cell and gene therapies. Nature Medicine 30, 1836–1846 (2024). https://doi.org/10.1038/s41591-024-03035-1
29. Kliegman, M., Zaghlula, M., Abrahamson, S. et al. A roadmap for affordable genetic medicines. Nature 634, 307–314 (2024). https://doi.org/10.1038/s41586-024-07800-7
30. Hope et al., 2022, *BMC Biology*: fluid shear stress enhances T cell activation through Piezo1. Useful for mechanobiology rationale
31. Sarna et al., 2024, *iScience*: sustained T cell activation in response to fluid shear stress. Useful if you want to strengthen the mechanical-force argument.
32. International Council for Harmonisation of Technical Requirements for Pharmaceuticals for Human Use. ICH Harmonised Guideline Q8(R2): Pharmaceutical Development. Step 4 version, August 2009.
33. International Council for Harmonisation of Technical Requirements for Pharmaceuticals for Human Use. ICH Harmonised Guideline Q11: Development and Manufacture of Drug Substances - Chemical Entities and Biotechnological/Biological Entities. Step 4 version, 1 May 2012.
34. European Medicines Agency. European Public Assessment Reports: Background and Context. European Medicines Agency.

Figure 1 | Optimization of static viral transduction and culture conditions in G-Rex

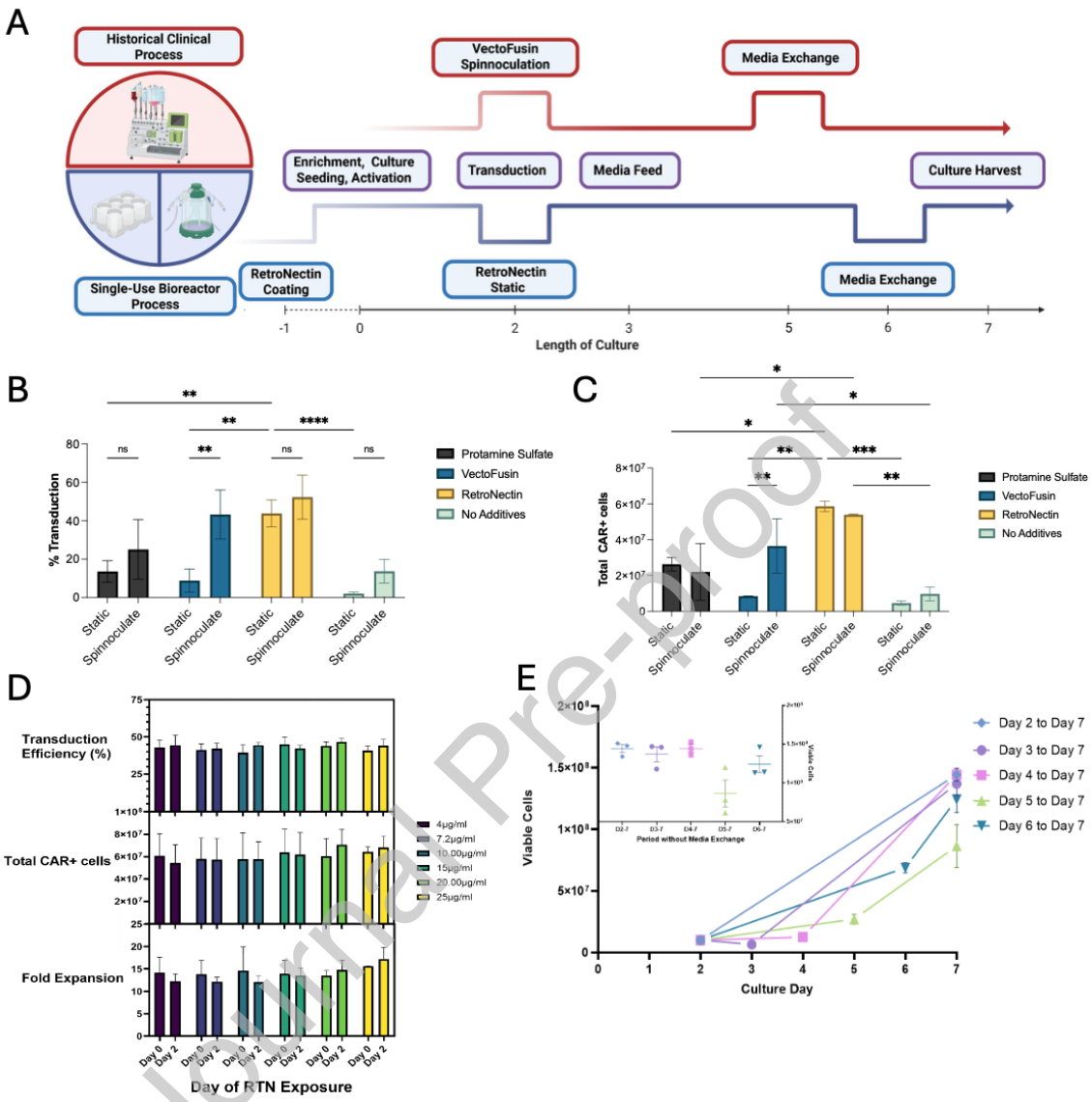

Figure 1 | Optimization of static viral transduction and culture conditions in G-Rex

a, Overview of the process-development strategy. The historical CliniMACS Prodigy-based GD2 CAR T-cell manufacturing process served as the clinically validated reference workflow. G-Rex-specific process parameters were initially evaluated using small-scale G-Rex 6M-well cultures, including static viral transduction, RetroNectin coating conditions, vessel retention, and media-exchange timing. The optimized conditions were subsequently translated to an integrated manufacturing-scale G-Rex 100M-CS workflow incorporating direct in-vessel $CD4^+/CD8^+$ enrichment, as evaluated in Figure 3. b, Transduction efficiency (TE) of GD2 CAR T cells following retroviral transduction under spinoculation or static conditions using Protamine Sulfate (PS), Vectofusin-1 (VF), or Retronectin (RTN) coating. c, Fold expansion at Day 7 across transduction enhancer conditions under spinoculation or static conditions. d, Effect of RetroNectin coating concentration and coating timing on transduction efficiency, total CAR-positive cell yield, and fold expansion at Day 7. For the Day 0 exposure condition (Day -1 Coating), G-Rex vessels were coated before activation on Day 0, and cells remained in the same vessel through transduction. For the Day 2 exposure

condition (Day 1 coating), cells were activated in an uncoated vessel and transferred on Day 2 into a separately coated vessel immediately before transduction. Bars represent mean ± s.d., N=3 donors. e, Total viable cell yield across culture period and endpoint (inset) at Day 7 following media exchange at indicated timepoints post-transduction (24–120 h) compared to undisturbed culture. Data represent mean ± s.d. from n = 3 independent donors. Statistical comparisons were performed using one-way ANOVA with correction for multiple comparisons unless otherwise indicated. Significance is denoted as *, $P < 0.05$, **, $P < 0.01$, ***, $P < 0.001$ and ****, $P < 0.0001$; ns, not significant.

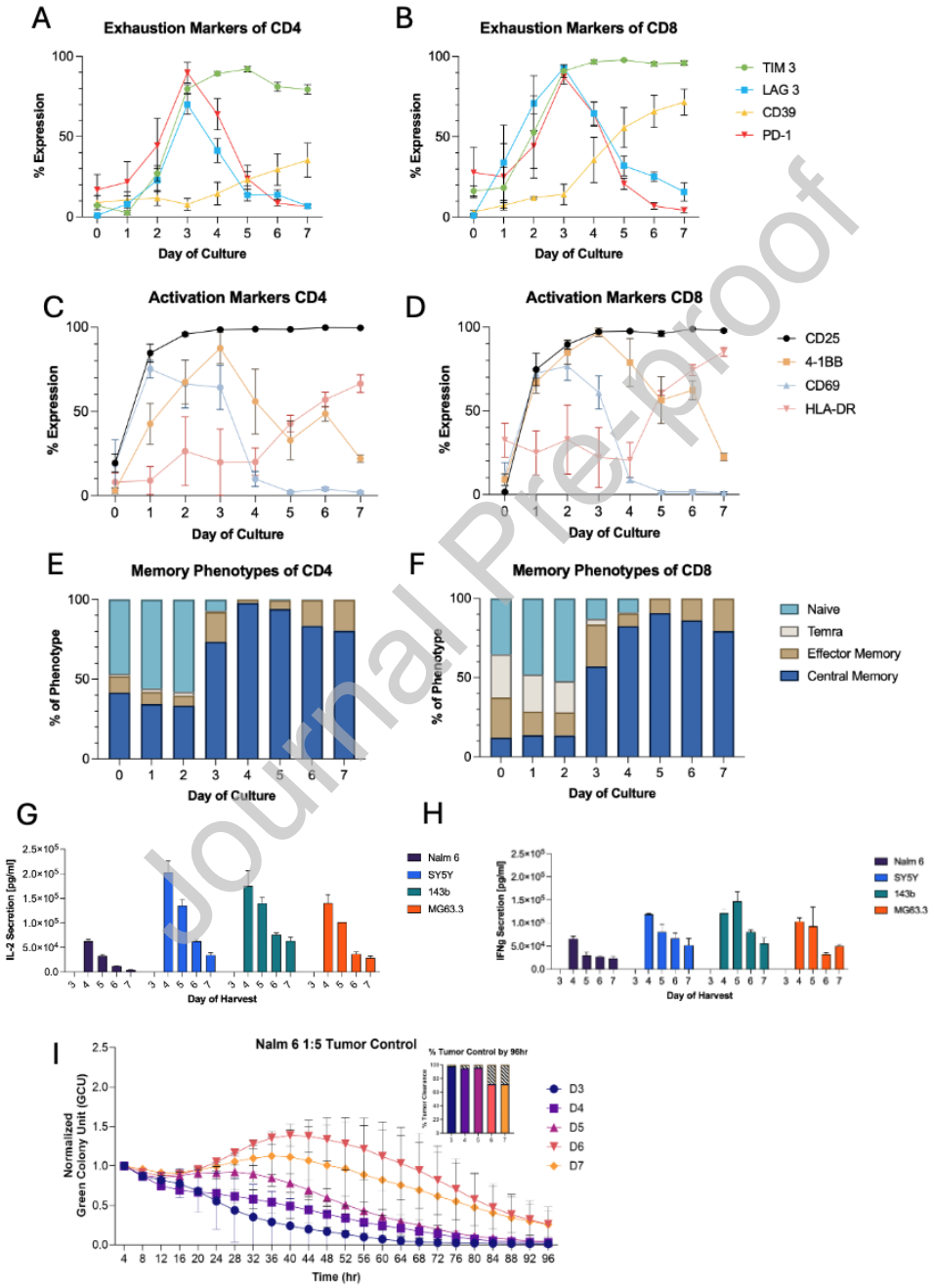

Figure 2 | Longitudinal phenotypic and functional characterization during G-Rex culture

a,b, Expression of immune checkpoint markers PD-1, LAG-3, CD39, and TIM-3 on $CD4^+$ (a) and $CD8^+$ (b) T cells across culture days. **c,d,** Activation marker expression (4-1BB, CD69, CD25, HLA-DR) across culture days **e,f,** Memory phenotype distribution (CD45RA, CCR7) demonstrating central memory (TCM; $CCR7^+CD45RA^-$) enrichment during culture. **g,h,** IL-2 and IFN-γ secretion following co-culture of CAR T cells harvested on the indicated culture days with GD2-expressing tumor target cells. CAR expression was measured at each harvest time point, and effector-cell inputs were normalized to 5×10^4 CAR-positive T cells per condition. GD2-expressing tumor cell lines included NALM-6-GD2, an engineered GD2-expressing B-cell leukemia model; SY5Y, a neuroblastoma cell line; and 143B and MG63.3, osteosarcoma cell lines used as GD2-positive solid tumor targets. I, Cytotoxic activity of CAR T cells harvested at indicated timepoints assessed by IncuCyte-based real-time killing assay, Y-axis: quantification of GFP signal from the tumor cells (GCU), inset: percent tumor control at end of study (96 hours), at each harvest timepoint. Data represent mean ± s.d. from n = 3 independent donors. Statistical comparisons were performed using repeated measures ANOVA with correction for multiple comparisons.

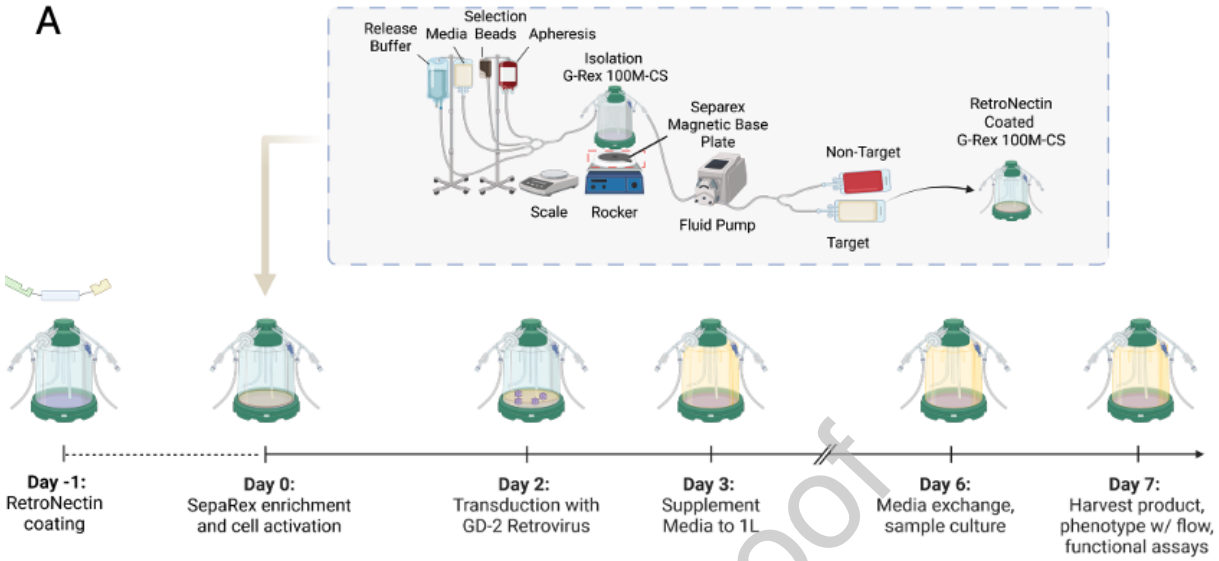

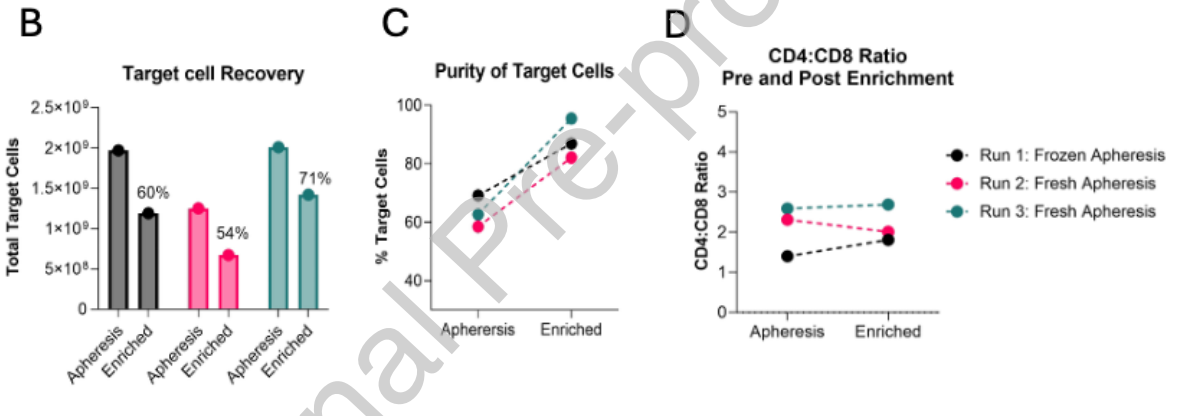

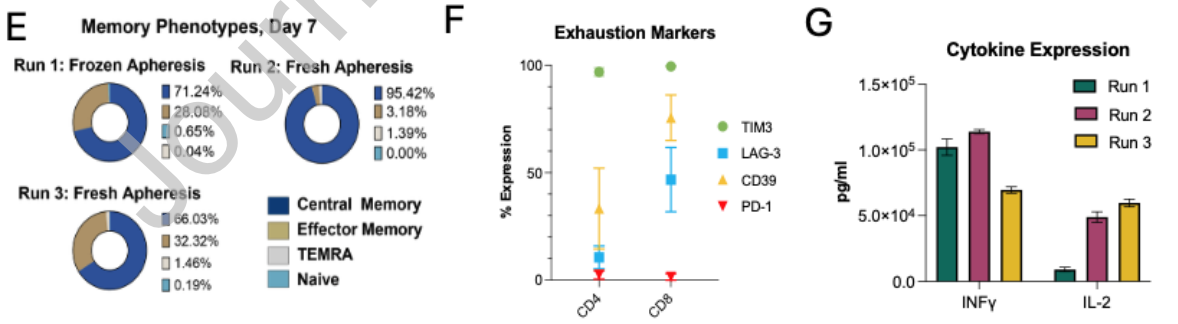

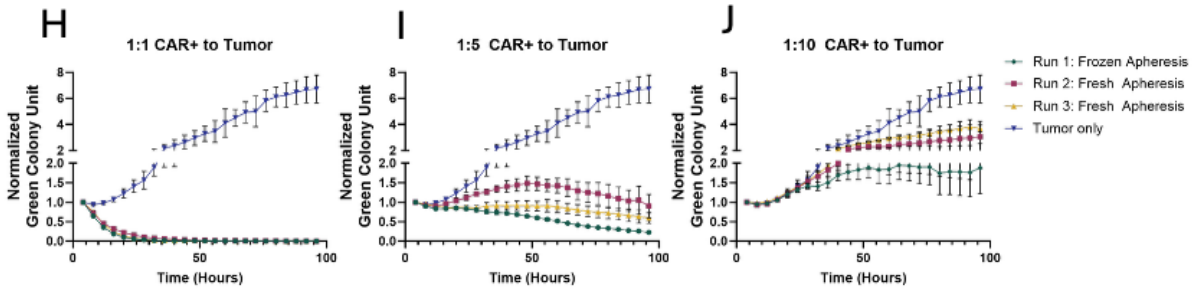

Figure 3 | Fully closed in-vessel CD4/CD8 enrichment enables end-to-end CAR T manufacturing and preserves product phenotype and function.

a, Schematic of the fully closed, in-vessel $CD4^+/CD8^+$ magnetic enrichment workflow performed directly within the closed-loop bioreactor. Leukapheresis material is introduced into the G-Rex vessel and combined with detachable CD4 and CD8 magnetic beads. The vessel is secured onto a magnetic base, enabling application of a magnetic field that immobilizes bead-bound target T cells onto the gas-permeable membrane surface while non-target cells are removed through controlled wash steps via a closed fluid transfer set. Following washing, the vessel is removed from the magnetic base to allow bead release in dissociation buffer. Reapplication of the magnetic field captures residual beads, permitting recovery of bead-free enriched $CD4^+/CD8^+$ T cells without transfer to a separate enrichment device. **b**, $CD4^+/CD8^+$ Target cell recovery following in-vessel enrichment for three independent manufacturing runs (Runs 1–3), shown as total recovered target cells and annotated with percent recovery for each run. **c**, Purity of target cells in the starting apheresis material and following enrichment for Runs 1-3, shown as percent target cells ($CD4^+$ and $CD8^+$ T cells) pre- and post-enrichment. **d**, Individual $CD4^+$ and $CD8^+$ T-cell frequencies before and after enrichment for each at-scale run. **e**, Memory phenotype distribution of the final CAR T cell products for Runs 1–3 (donut plots), shown as percent composition of indicated memory subsets. **f**, Expression of exhaustion/activation-associated markers in the final product, shown for $CD4^+$ and $CD8^+$ compartments (markers indicated in legend). **g**, Cytokine production by manufactured CAR T cells following stimulation/co-culture, shown as IFN-γ and IL-2 for three independent replicates (as plotted). **h-j**, Real-time cytotoxicity kinetics of anti-GD2 CAR T cells co-cultured with GD2-expressing tumor target cells at effector-to-target (E:T) ratios of 1:1 (**h**), 1:5 (**i**), and (**j**) 1:10 over the indicated time course (hours), displayed as mean ± s.d. across replicates (as plotted). Data correspond to three independent manufacturing runs.

Table 1. Comparison of T Cell Enrichment metrics Across Platforms

Metric	G-Rex™ Direct Enrichment (N = 3)	CliniMACS Prodigy (N=68)	Dynacellect (N=3)
Enrichment Bead Type	CTS™ CD4/CD8 Detachable DynaBeads™	Clinimacs® CD4, CD8 Reagent	CTS™ CD4/CD8 Detachable DynaBeads™
Recovery (%)	61.6 ± 8.6	73.2 ± 17.1	64.24 ± 15.2
Purity of $CD4^+/CD8^+$ Cells (%)	88.2 ± 6.8	94.1 ± 3.8	93.3 ± 4.5
CD3+ T Cells at Harvest (%) (% of culture)	>96%	>96%	>96%
Processing Time	2.5 hours *independent of input cell load*	3-4 hours *dependent on input cell load*	2.5 hours *independent of input cell load*
Automation Level	Manual	Fully automated	Semi-automated

Table 2. Comparison of CAR T Manufacturing Metrics

Metric	G-Rex™ At-Scale (N = 3)	Clinical GD2 (N = 68) CliniMACS Prodigy, NCT04196413	
Culture Duration	7-day Expansion	7-day Expansion	
Transduction Efficiency	62.3 % ± 5.1 %	51.1 % ± 29.4 %	ns
Fold-Expansion	26.8 ± 4.7-fold	24.1 ± 33.5 fold	ns
$CD3^+$ Purity at Harvest	>96 %	>96 %	ns
Viability at Harvest	94.0 % ± 3.2 %	94.3 % ± 3.1 %	ns
Memory Markers	**G-Rex™ At-Scale (N = 3)** *Healthy Donors*	**CliniMACS Prodigy (N = 19)** *Clinical*	

		Patient Data NCT04196413	
Stem Cell Memory Subset (TSCM, %) (CAR+ CD4+)	2.662 % ± 0.7341 %	2.36 % ± 2.748 %	ns
Central Memory Subset (TCM, %) (CAR+ CD4+)	76.49 % ± 18.19 %	69.68 % ± 19.96 %	ns
Effector Memory Subset (TEM, %) (CAR+ CD4+)	20.50 % ± 17.08 %	27.64 % ± 19.69 %	ns
Terminally Differentiated Effector Memory Subset (TEMRA, %) (CAR+ CD4+)	0.3612 % ± 0.3665 %	0.3232 % ± 0.3963 %	ns
Stem Cell Memory Subset (TSCM, %) (CAR+ CD8+)	2.917 % ± 3.824 %	1.867 % ± 1.794 %	ns
Central Memory Subset (TCM, %) (CAR+ CD8+)	68.53 % ± 26.46 %	76.38 % ± 15.79 %	ns
Effector Memory Subset (TEM, %) (CAR+ CD8+)	28.27 % ± 22.99 %	21.50 % ± 15.51 %	ns
Terminally Differentiated Effector Memory Subset (TEMRA, %) (CAR+ CD8+)	0.2725 % ± 0.4232 %	0.2318 % ± 0.4047 %	ns
Exhasution Markers	**G-Rex™ At-Scale (N = 3)** *Healthy Donors*	**CliniMACS Prodigy (N = 19)** *Clinical Patient Data NCT04196413*	
CD39+ % (CAR+ CD4+)	31.62 % ± 17.60 %	29.19 % ± 21.63 %	ns
LAG3+ % (CAR+ CD4+)	6.312 % ± 5.398 %	6.097 % ± 5.189 %	ns
PD-1+ % (CAR+ CD4+)	2.451 % ± 2.021 %	15.15 % ± 7.920 %	** **
TIM3+ % (CAR+ CD4+)	96.83 % ± 1.972 %	98.89 % ± 0.9536 %	ns
CD39+ % (CAR+ CD8+)	74.12 % ± 9.558 %	64.27 % ± 21.05 %	ns
LAG3+ % (CAR+ CD8+)	40.45 % ± 15.23 %	4.506 % ± 4.361 %	ns
PD-1+ % (CAR+ CD8+)	1.505 % ± 1.591 %	13.23 % ± 8.065 %	** **
TIM3+ % (CAR+ CD8+)	99.43 % ± 0.3215 %	99.83 % ± 0.1522 %	ns

GD2 clinical trial (NCT04196413) enrolled pediatric patients with diffuse intrinsic pontine glioma (DIPG) and spinal diffuse midline glioma (sDMG).
The phenotypic data were generated using drug product retains from clinical manufacturing runs

Table 3. Comparative cost Analysis of CAR T manufacturing Platforms

Cost Category / Parameter	G-Rex™–Based Workflow	Automated Platforms
Capital Equipment	$1.1K per G-Rex™ module, $30K in incubators	$150K–$300K per instrument
Consumables Cost per Batch	$14-16K	$21-23K
Process Complexity	Low; single-use, modular system enables custom protocols	High; requires trained operators; fixed protocol
Throughput	Easily parallelized; add reactors per patient	Typically 1 patient per unit
Workflow Automation	Manual with minimal intervention	Fully automated, frequent manual troubleshooting and intervention
Decentralized Manufacturing Feasibility	High - compatible with academic and regional hospital GMP settings	Limited - high costs and complex training limit adoption in small sites
Best Use Case	Academic centers, decentralized and centralized production	High-volume centralized GMP sites